Research Article

Márta Polgári*, Ildikó Gyollai, Szaniszló Bérczi, Miklós Veres, Arnold Gucsik, and Elemér Pál-Molnár

Microbial mediation of textures and minerals – terrestrial or parent body processes?

https://doi.org/10.1515/astro-2019-0004
Received Jan 26, 2018; accepted Jul 11, 2018

Abstract: Evolution of chondritic parent body is influenced by thermal, impact metamorphism and aqueous alteration, studied in Mező-Madaras, Knyahinya, Mócs and Nyírábrány in aspect of high resolution *in situ* textural, mineralogical and organic geochemical characteristics, using optical microscopy, FTIR-ATR and Raman spectroscopy. Our observations focused on Fe-containing opaque grains, glass, olivines and pyroxenes, which were well populated by micrometer-sized microbial filamentous elements in their boundary region within matrix and inside the minerals resembling mineralized microbially produced textures (MMPT), affecting 70-80 vol% of samples. In MMPT iron oxides (ferrihydrite, goethite), olivine, montmorillonite, kandite minerals and various hydrocarbon compounds were identified.

(1) Data confirmed dense and invasive terrestrial microbially mediated contamination in the chondrites, supported by microtexture, micromineralogy and embedded organic compounds. As the classical transformation processes are supposed nowadays to have been happened on the parent bodies, a contradiction arose: how could it be that these classical products are manifested in microbially mediated texture?
(2) Based on terrestrial analogies, microbial mediation is a sudden process comparing to geological times, very ancient, widespread and occur in various environments under determined conditions. It can consume previous and also produce new minerals. After formation, MMPT can survive billions of years proposing occurrence on parent bodies.

Keywords: chondrite, minerals, alteration, microbial, exobiology, Fe-oxidizing microbes

1 Introduction

Most of the meteorite falls (85%) consist of chondritic stone meteorites, which preserve primordial evolutionary stages of the Solar System materials in condensed state. As fragments of asteroidal sized parent bodies, the chondrites preserve several parent body transformations.

Chondritic material evolution has been first deduced from the thermal metamorphism caused by the heating up of short living radionuclides in the chondritic asteroidal sized parent body. This process has been resulted in onion-layered body with higher temperatures in the core regions and lower temperatures at the margin of the body. The metamorphic events started from parent bodies with different initial compositions (E, H, L, LL, C) first distinguished by their mineralogy and chemistry and groups were named by their total iron content to H (high) and L (low) (Urey & Craig, 1953), which system was later extended to the E, H,

Corresponding Author: M. Polgári: Research Centre for Astronomy and Geosciences, IGGR, HAS, 1112 Budapest, Budaörsi str. 45, Hungary; Eszterházy Károly University, Dept. of Natural Geography and Geoinformatics, 3300 Eger, Leányka str. 6, Hungary;
Email: rodokrozit@gmail.com
I. Gyollai: Research Centre for Astronomy and Geosciences, IGGR, HAS, 1112 Budapest, Budaörsi str. 45, Hungary;
Email: gyildi@gmail.com
Sz. Bérczi: Eötvös University, Dept. of Materials Physics, Cosmic Materials Space Res. Group, H-1117 Budapest, Pázmány P. str. 1/a, Hungary;
Email: berczi szani@caesar.elte.hu
M. Veres: Wigner Research Centre for Physics, HAS, 1121 Budapest, Konkoly-Thege M. str. 29-33, Hungary;
Email: veres.miklos@wigner.mta.hu
A. Gucsik: Eszterházy Károly University, Dept. of Natural Geography and Geoinformatics, 3300 Eger, Leányka str. 6, Hungary; Wigner Research Centre for Physics, HAS, 1121 Budapest, Konkoly-Thege M. str. 29-33, Hungary; University of Johannesburg, Department of Geology, 2600 Auckland Park, Johannesburg, South Africa;
Email: ciklamensopron@yahoo.com
E. Pál-Molnár: University of Szeged, Dept. of Mineralogy, Geochemistry and Petrology, 6722 Szeged, Egyetem str. 2, Hungary; Email: palm@geo.u-szeged.hu
The first three authors have contributed equally to this work

L, LL, and C main groups of chondrites (enstatite (E), carbonaceous (C), etc., Mason, 1963). The textural sequence of petrologic types of chondrites formed in thermal metamorphism has been formulated by Van Schmus & Wood (1967). The thermal evolutionary paths are similar for ordinary chondrites (OC) from 3 to 6 petrologic types.

The system of van Schmus-Wood sequence of petrologic types (1967, including petrologic classes) has been modified by McSween's (1979). This modification was based on the suggestion that metamorphism and aqueous alteration could have been separated processes. On the one hand, the metamorphism means heating up of asteroidal parent bodies forming layers of chondrites with type 3-6 (from outer shell of type 4 to the inner shell of type 6 in an onion-shell model parent body), and the corresponding thermal range is 400-1000°C. During this process diffusion in the solid state chondrite homogenized the textural differences and coarsened the mineral texture with the increasing temperature. On the other hand, aqueous alteration means a process that operated mainly on carbonaceous chondritic asteroidal parent bodies at low temperatures (0-200°C). In this process water was a stable constituent of the chondritic texture producing hydrated minerals (phyllosilicates) and salts (McSween, 1979; Zolensky & McSween, 1988; Scott *et al.*, 1997).

The aqueous alteration predated the thermal metamorphism, which partly washed out its mineral products. However, the bleached regions of the chondrules preserved some alteration characteristics in enrichment of alkalias, especially Na content, the changes of the Fe content and some phyllosilicates, too (Kurat, 1969; Grossman *et al.*, 1997, 2000; Grossman & Brearley, 2005).

The conclusions of the alteration processes in unequilibrated ordinary chondrites (UOC) were, that three main steps are common in UOC matrix and chondrule development: 1) aquaeous alteration 2) dehydration, and 3) a mild thermal metamorphism (Hutchison *et al.*, 1987). Studies continued in the last 15 years on type 3 chondrites (UOC, CV and CO chondrites, *i.e.* Semarkona, Bishunpur, Krymka, Sharps, Allende and Bali) and confirmed in more details that both chondrules and matrices were affected by lighter or stronger aqueous – involving iron-alkali-halogen migrating – alterations or metasomatism. Specific alteration forms were observed in the form of thick "bleached" zones at chondrule surfaces and along cracks inside chondrules (Grossman *et al.*, 1997), or as a significant component of amorphous material in matrices produced by metasomatism (Brearley, 1997), or as extensive alteration and dehydration products (Scott *et al.*, 1997). Most of the affected phases were in the extremely fine-grained matrix, or at the porous regions, in altered patches, veins and mesostasis in the chondrules.

So, investigation during the last decades has resulted in details on the mineralogical, elemental, and isotopic data and distribution of unequilibrated ordinary chondrites (UOC) (Van Schmus & Wood, 1967; Kurat, 1969; Grossman *et al.*, 1997, 2000; Grossman & Brearley, 2005; Menzies *et al.*, 2005). However, open questions and contradictions arose in several measurements (SI.1A - General main interpretations/conclusions, questions and contradictions (A) concerning UOC based on selected references and the proposed interpretation and answers based on recent study (B)):

(1) why are there selective enrichments of some elements (alkali and Fe enrichments among others);
(2) what is the cause of the changes of element distributions, the element inhomogeneity, the redistribution of elements (selective enrichments and decreases) in matrix, in marginal parts of chondrules, forming zonation;
(3) why are compositions not in equilibrium with the coexisting minerals;
(4) why are zoning profiles similar for elements with very different diffusion coefficients and condensation temperatures;
(5) why can we observe the survival of amorphous material which represents a highly disordered metastable state;
(6) the presence of CAI-like material among precursors for Al-rich chondrules is in apparent conflict with the lack of evidence for the melting of CAIs that occur outside chondrules, etc.

Models for solution of the above contradictions have also been proposed, based on (i) the requirement of the occurrence of pre-existing minerals and unknown enrichment mechanisms; and (ii) the suggestion of an interface-coupled dissolution–re-precipitation mechanism during metasomatism.

The origin of organic compounds that are often found in carbonaceous chondrites (CC) has also been studied. After the pioneering discoveries that living organisms might have been present in CC, in chondrites the microbial involvement is a living topic in meteoritics, again accompanied by contradictions (Claus & Nagy, 1961; Nagy *et al.*, 1963). Continuous studies have revealed the presence of various prokaryotes and filamentous cyanobacteria in CI1 chondrites (Oró *et al.*, 1971; Engel & Nagy, 1982; Hoover *et al.*, 1998; Hoover, 2012). Further chemical characteristics of organic material – such as biomolecules – have been determined, and interpreted as the breakdown remnants of

Table 1. The studied meteorites and their characterization (Eötvös University Meteorite Collection, Budapest) (Grady *et al.*, 1982; Graham *et al.*, 1985)

Name	Locality	GPS data	Observed fall	Classification	Type	Fe_{tot}-wt. %	C_{tot} wt. %	$\delta^{13}C$ ‰	Pb/Pb age Ga
Mező-Madaras	Mădăras, Mures County (Romania)	46°36′N; 24° 26′E	4, Sept, 1852	Brecciated, xenolitic chondrite	L3,7	21.6	0.45	−22.6	4.55
Knyahinya	Ukraina	48°54′N; 22°24′E	9, June, 1866	Brecciated chondrite	L/LL5	20.15	No data	No data	4.55
Nyírábrány	Hajdú-Bihar County (Hungary)	47°32′39.66″N; 22°00′51.88″E	17, July, 1914	Chondrite	LL5/L6	20.38	No data	No data	No data
Mócs	Mociu, Cluj County (Romania)	46°47′45″N; 24°02′07″E	3, Febr, 1882	Chondrite	L6	21.81	No data	No data	4.55

Shock stage: S5, mechanical twinned pyroxenes, deformation twin lamellae, weak mosaicism, planar deformation

cyanobacteria originating from the meteorite parent body. A parallel line of potential microbial evidence was gained from Martian meteorites (McKay *et al.*, 1996). Efforts to interpret extraterrestrial life have also been made, but are still being debated as concerns (i) preservation opportunities of organic matter (high T); (ii) terrestrial contamination problems; (iii) survival time, Ga; and (iv) the generally accepted abiogenic origin.

In this paper we show that in the L and LL chondrites we studied (Mező-Madaras, Knyahinya, Mócs and Nyírábrány), the texture had been affected deeply by primordial syngenetic putative microbial mediation and the advancing microbial activity caused also gradually increasing phyllosilicate formation. Earlier, these effects were concluded to have been the result of aqueous alteration and metamorphous effects along the chondrite transformations sequence from L3 to L6.

The accepted evolution model of chondritic parent body asserts that bodies were influenced by thermal and impact metamorphism and aqueous alteration, which have been studied in our Mező-Madaras, Knyahinya, Mócs and Nyírábrány samples in aspect of high resolution *in situ* textural, mineralogical and organic geochemical characteristics, using optical microscopy (OM), FTIR-ATR and Raman spectroscopy. Our observations (OM) focused on the Fe-containing opaque grains, glass, olivines and pyroxenes, which were well populated by micrometer-sized microbial filamentous elements (clusters) in their boundary region within matrix and inside the minerals resembling mineralized microbially produced textures (MMPT), affecting up to 70-80 vol.% of the samples. In the MMPT iron oxides (ferrihydrite, goethite), olivine, montmorillonite, various hydrocarbon compounds, and also kandite minerals were identified.

The present study aims at and offers a basically new aspect and complex interpretation series of the new dataset.

2 Samples

Historical meteorite events in the Carpathian Basin produced several important falls (Meteorite Catalogue London) (Graham *et al.*, 1985). Our Mező-Madaras, Knyahinya and Mócs meteorites were distributed into larger collections and later played a role in the meteoritic discipline, mainly in the thermal metamorphism model of the chondritic parent body evolutionary processes. Data on the studied meteorites are given in Table 1, Figure 1.

The brecciated and xenolithic nature of Mező-Madaras was observed as early as in the late 19th century (Meunier, 1871), where the mostly granular, porphyritic, barred and radial chondrules have sharp chondrule boundaries. In Knyahinya, Nyírábrány and Mócs the boundaries of the chondrules are more obscured, while the matrix is partly recrystallized, with gradually grown mineral grains in the matrix.

3 Methods

Petrographic structural-textural studies were undertaken on 4 thin sections using a Nikon ECLIPSE 600 optical petrographic microscope (OM) in Budapest, IGGR-RCAES-HAS, Hungary.

The IR measurements were utilized by a Bruker VERTEX 70 Fourier transform infrared spectrometer equipped

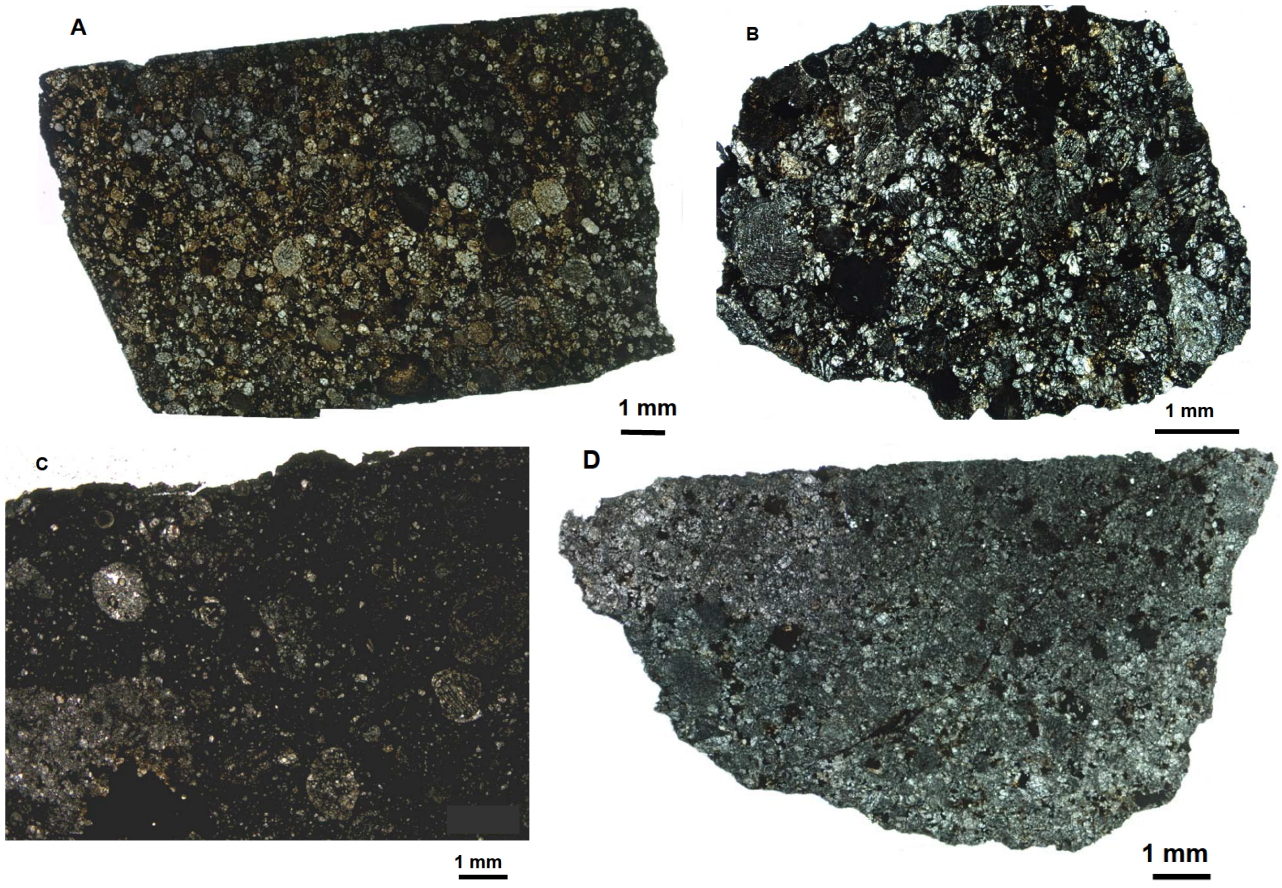

Figure 1. Thin section photos of Mező-Madaras (A), Knyahinya (B), Nyírábrány (C) and Mócs (D) chondrites.

with a Bruker HYPERION 2000 microscope with a 20x ATR objective and MCT-A detector, with spatial resolution of 2 μm. During ATR analysis, the samples were contacted with a Ge crystal (0.5 micron) tip on the selected 1 N pressure. The measurement was conducted for 32 seconds (32 scans) in the 600–4000 cm^{-1} range with 4 cm^{-1} resolution. Opus 5.5 software was used to evaluate the data. To avoid the interpretation of environmental conditions of the measurements in the samples, the spectra of dichloromethane, glass rode were used as background.

Raman spectra were recorded using a Renishaw RM-2000 Raman spectrometer attached to a Leica DM/LM microscope with a 785 nm diode laser as excitation source (8 mW power at the excitation spot) and spot diameter of 1 micron at the Wigner Research Centre for Physics, HAS, Budapest, which is suitable to detect both of inorganic and organic phases of samples. Identification of minerals was made with the RRUFF Database (Database of Raman – spectroscopy, X-ray diffraction, and chemistry of minerals: http://rruff.info/). Contamination by epoxy glue was taken into consideration. The baseline correction and peak fitting was done by GRAMS software in HAS Wigner Institute of Physics.

4 Results

4.1 High resolution optical microscopy

Our observations (OM) focused on the iron-containing opaque grains, glass, olivines and pyroxenes, which were well populated by micrometer-sized microbial filamentous elements and clusters in their boundary region within the matrix and inside the minerals. A diverse suite of complex filamentous micro-textures was extensively deeply embedded in the matrix, in the fractures and also in the inner phase of the chondrules and minerals (up to 70–80% of the sections were affected by microbial mediation).

All thin sections showed signs of Fe mobilization and oxidation (brown haloes around mineral grains, brown filaments, Figure 2, SI 2 - Microtexture of chondrites (thin sections by optical rock microscopy)).

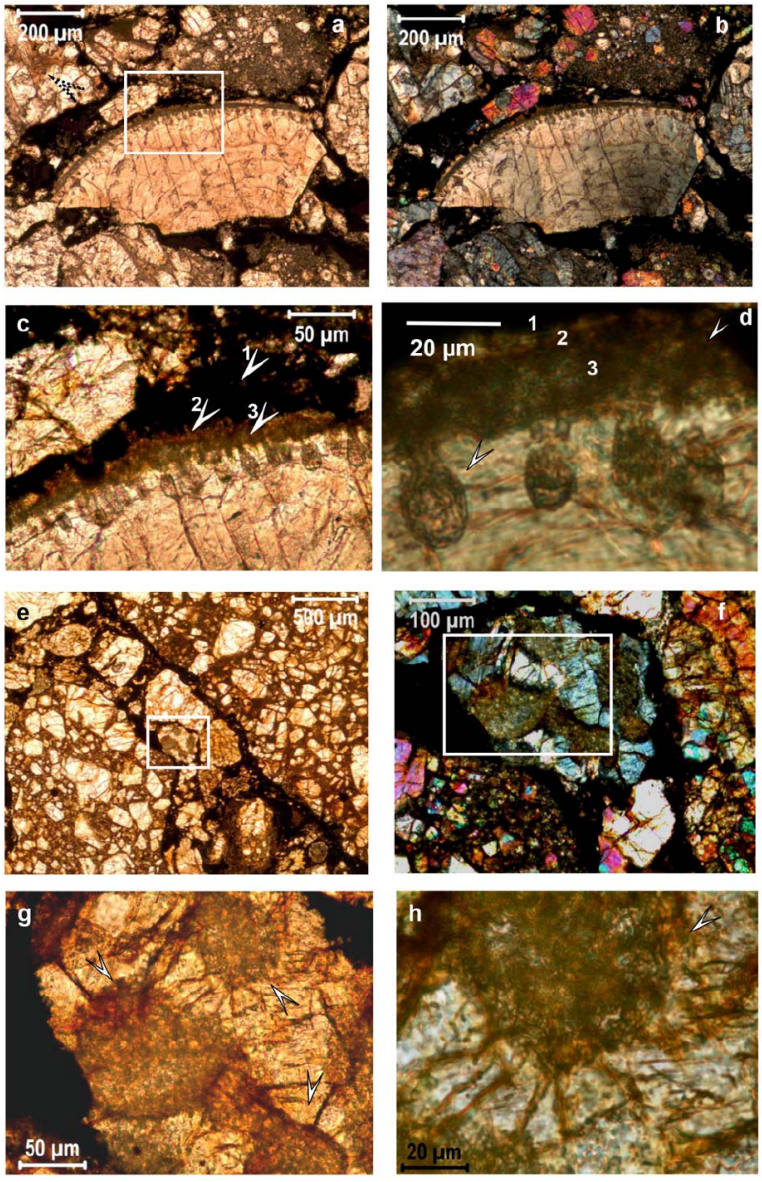

Figure 2. Characteristic microtexture of chondrites. (a) characteristic microtexture of Mező-Madaras chondrite containing chondrules (broken one in the centre), and olivine and pyroxene mineral clasts embedded in opaque fine-grained matrix (1N), dashed arrow show Fe-mobilization; (b) the crossed N photo of (a); (c) higher magnification of marked area on (a), arrows show transition from opaque matrix (1) towards the broken chondrule (2- brown part and 3- greenish-brown part), opaque matrix (1) consists of nanocrystalline graphite, weathered olivine and pyroxene, dickite and montmorillonite (SI. 4 - Raman spectroscopy - Mező-Madaras (MM) meteorite), brown part is weathered olivine, pyroxene, ferrihydrite, montmorillonite and dickite (2), part (3) consists of organic matter, ferrihydrite, montmorillonite, kaolinite and halloysite determined by Raman spectroscopy (SI. 4 - Raman spectroscopy - Mező-Madaras (MM) meteorite); (d) higher magnification of (c), parts 2 and 3 show characteristic microtexture of the contact zone between the chondrule and the matrix resembling filamentous microbial morphology with pearl necklace-like inner texture and bubble-like microbial colonies (organic matter, olivine, kaolinite, dickite, ferrihydrite, montmorillonite and nontronite) invading toward the inner part of the chondrule (weathered Fe-Mg-silicate, dickite, organic matter); (e) characteristic microtexture of Mező-Madaras chondrite (1N); (f) higher magnification of marked area on (e) (crossed N); (g) higher magnification of marked area on (f) (1 N) with intense microbially mediated parts showed by arrows; (h) higher magnification of (g) showing intense microbially mediated parts (arrow); (i) characteristic microtexture of Mező-Madaras chondrite (crossed N); (j) higher magnification of marked area on (i) (1N), the fractures of the quartz are embedded by filamentous microbial forms; (k) characteristic microtexture of Knyahinya chondrite (1N), dashed arrows show Fe-mobilization; (l) higher magnification of marked area on (k) (1N), showing intense microbially mediated parts (arrow); (m) opaque part with Fe-mobilization around (dashed arrows) in Mező-Madaras chondrite with microbial signatures (arrows)(the opaque part is trolitite or metal Fe)(1N, transmitted light); (n) intense microbially mediated parts showed by arrows are embedded in opaque part (reflected light).

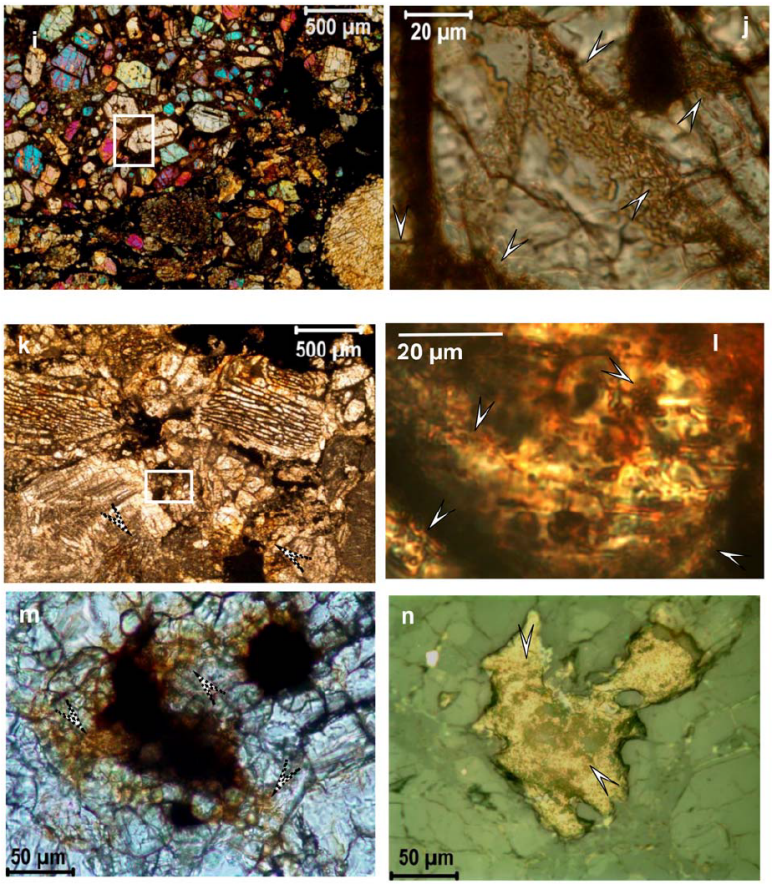

Figure 2. ... continued

Well-preserved and mineralized remains of diverse filaments with pearl necklace-like, vermiform inner signatures interpreted as mineralized remains of prokaryotes (MMPT) embedded in the stone meteorites were observed for the first time in the thin sections at higher magnifications, together with a bubble-like invasion front (consisting of a similar filamentous morphology) towards a broken chondrule. The diameter of the mineralized filaments is around 0.5–1 µm, with variable length (Figure 2).

Mező-Madaras represents well preserved unaltered chondrules and minerals, but the mineralized microbial signature is basically embedded in this meteorite, too.

In Knyahinya, Nyírábrány and Mócs not only had the boundaries of the chondrules become obscured but large regions had been transformed into an invisible greenish-gray clay-like non-transparent phase. Some chondrules were recrystallized and the grain size increased in the course of thermal metamorphism, but the iron-containing minerals were also populated by micrometer-sized microbial clusters (Figure 3). The opaque grains also show signs of microbial mediation (SI 2E - Microtexture of chondrites (thin sections by optical rock microscopy)).

4.2 IR spectroscopy

Iron-oxidizing microbial mediation in the Mócs sample was measured by ATR-FTIR spectroscopy. The measuring **area 1** is around a bio-degraded region of opaque (troilite) grains surrounded by olivine (Table 2, Figure 4, SI 3 - ATR-FTIR spectroscopy results of Mócs meteorite). The measuring points of iron-oxidizing microbial structures have a mixed composition containing iron oxides (ferrihydrite 830, 930, 950 cm^{-1}) and goethite (670 cm^{-1}) (Glotch & Rossman, 2009), olivine (860, 970–995 cm^{-1}) (Matrajt *et al.*, 2005), and montmorillonite (625, 838–845–850, 880–890, 1005–1010, 1045, 1100–1110 cm^{-1}) (Madejova & Komadel, 2001). The ATR-FTIR microscopy is applicable proving the biogenicity of bacterial structures by the detection of hydrocarbon peaks at 720 cm^{-1} (long chain hydrocarbon), 1550–1650 cm^{-1} (C-O, C-O-C diene) (Rajasekar *et al.*, 2006; Parikh & Chorover, 2006), and peak groups of 2955, 2923, 2855 cm^{-1} (C-H stretching of aliphatic hydrocarbons) (Rajasekar *et al.*, 2006). The presence of olivine and montmorillonite spectra proves the weathering of olivine, while the appearance of ferrihydrite corresponds to bacterial originated remobi-

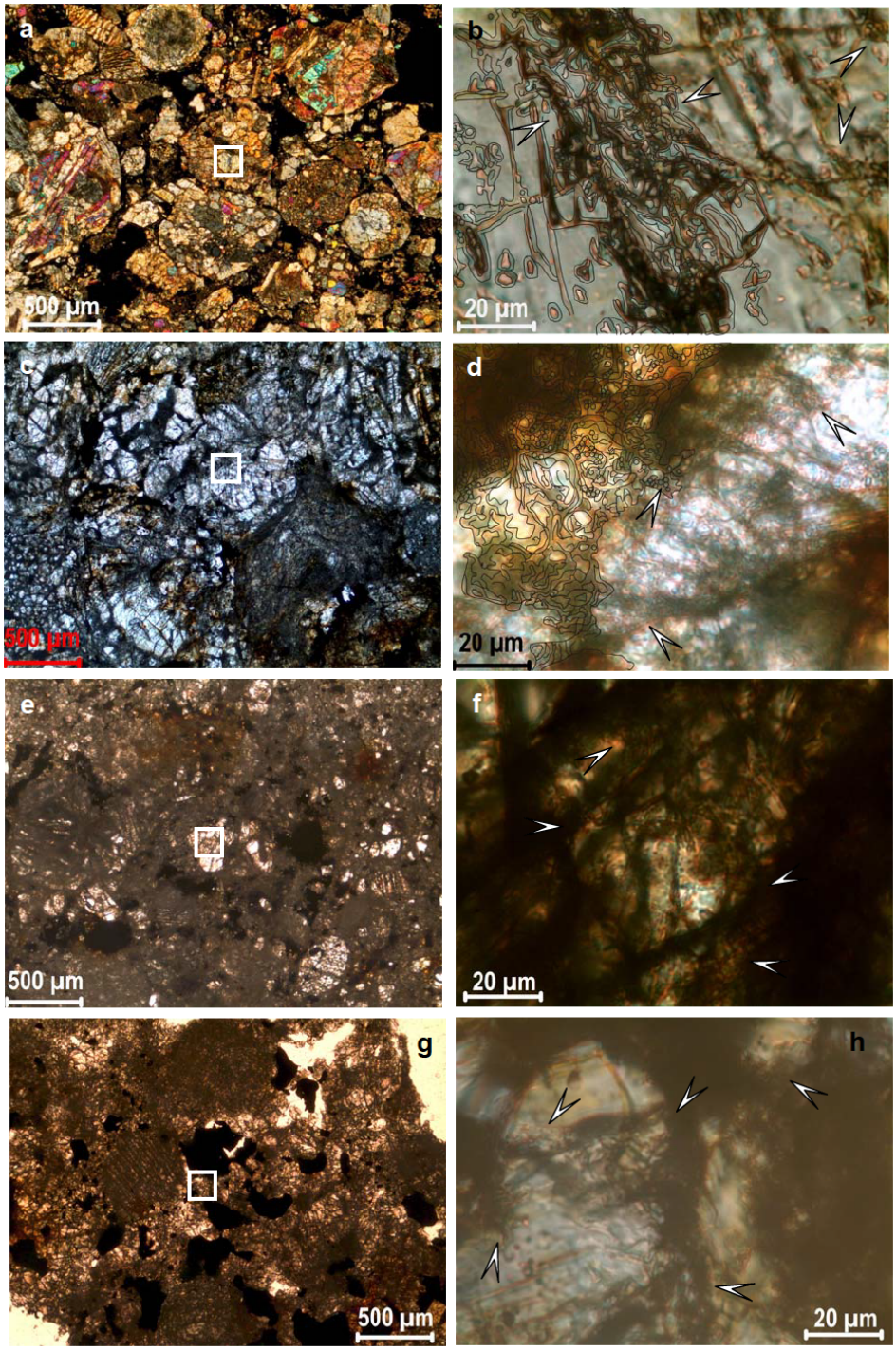

Figure 3. Microbial alteration sequence as alternative opportunity near thermal metamorphic sequence of the L-group chondrites (a-b)-Mező-Madaras L3.7, (c-d)-Knyahinya L/LL5, (e-f)-Nyírábrány LL5/L6, (g-h)-Mócs L6. We can observe how the sharp edges of chondrules gradually become fuzzy via homogenization caused by more and more intense clay formation from L3 to L6 (a, c, e, g), which process is called as Oswald-maturing in solid state physics for thermal metamorphism. (b, d, f, h) show filamentous microbial morphology with pearl necklace-like inner texture of colonies embedded in all chondrites of the marked areas (arrows). Optical rock microscopy, transmitted light 1N, except (a) which is crossed N. Some features in photos (b, d) were graphically enhanced for better recognition of MMPT due to low contrast of the photographs.

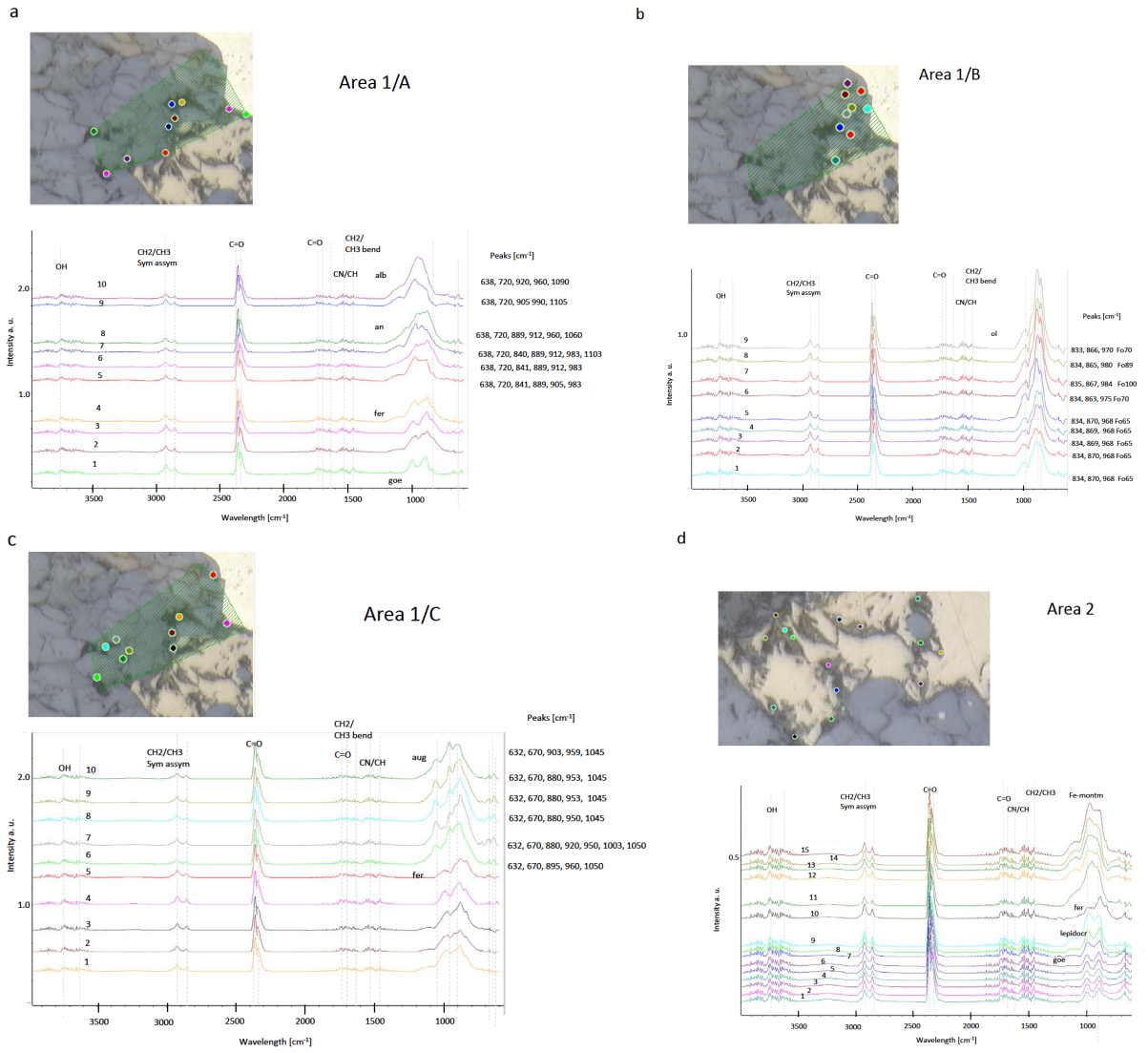

Figure 4. ATR-FTIR spectroscopy results of Mócs meteorite. Measuring Area 1 (a, b, c) is around bio-degraded area of opaque (troilite) grains (light phase), which are surrounded by olivine (spectrum groups A, B, C). The measuring points of iron-oxidizing bacterial structures have a mixed composition containing iron oxides (ferrihydrite and goethite), olivine, montmorillonite and hydrocarbon peaks (long chain hydrocarbon, C-H stretching of aliphatic hydrocarbons, etc.); Area 2 (d) represents opaque (troilite) phase, which contain montmorillonite, iron oxides and hydrocarbons. The IR vibrations of isoprenoids were also detected. Abbr: (a) alb-albite, an-anortite, fer-ferrihydrite, goe-goethite; (b) ol-olivine; (c) aug-augite, fer-ferrihydrite; (d) Fe-montm-Fe-montmorillonite, fer-ferrihydrite, lepidocr-lepidocrocite, goe-goethite.

lization of iron from iron rich olivine and troilite. Peaks in the region of 3600–3800 correspond to O-H stretching in phyllosilicates (Madejova & Komadel, 2001).

The peaks of montmorillonite were interpreted following (Madejova & Komadel, 2001), where also vibrations of iron oxides were described (Glotch & Rossman, 2009). The IR spectrum group B in area 1 (Figure 4) is measured in olivine, which consists of 3 major vibrations: v1 at 830 cm^{-1} (symmetric stretching), v2 at 860 cm^{-1} and 960–990 cm^{-1} (split Si-O stretching mode) (Hamilton, 2010). The peak at 675 belongs to goethite. The composition of olivine was estimated by calibration of Lane *et al.* (2011), which is Fo65-Fo70, near troilite and iron oxides, and varies between Fo89.5-Fo100 in normal olivine, far from opaque minerals. The Fe-rich olivine have broader peaks with lower intensity, whereas Mg-rich olivine have intense, sharp bands. According to Markovski *et al.* (2017), the biomediated minerals have higher Fe content, and vibration bands are broader, which is signature to distinguish minerals by abiogenic and biogenic origin.

The spectrum group C/spectra 1-4 (Figure 4) is olivine with only major doublet vibrations of olivine (830 cm^{-1}, 865

Table 2. Distribution of mineral and organic matter composition in Mócs meteorite determined by FTIR-ATR spectroscopy

		Sample ID	Area 1 A	Area 1 B	Area 1 C	Area 2
		Total No. of spectra→	10	9	10	15
Mineral phase	**References**	**Wavelength [cm^{-1}]**				
Olivine	Hamilton 2010	833, 864, 930sh, 986		9		
Augite	Dyar 2011	649, 705, 729, 848, 920, 1003, 1055			5	
Albite	Müller *et al.*, 2014	798, 950, 1000	2			
Anorthite	Müller *et al.*, 2014		4			
Ferrihydrite	Glotch & Rossman, 2009	692, 878, 3400	3		5	1
Lepidocrocite	Glotch & Rossman, 2009	602, 748, 895, 1023				2
Goethite	Glotch & Rossman, 2009	798, 910	1			6
Fe-montmorillonite	Madejova & Komadel, 2001	623, 748, 914, 989				6
Organic compounds						
d CH2	Parikh & Chorover, 2006	1454-1482	10	9	10	15
C-N, CH deformation	Parikh & Chorover, 2006	1526	10	9	10	15
C-N N-H amide II	Parikh & Chorover, 2006	1540-1550	10	9	10	15
C=C asym. Stretch	Parikh & Chorover, 2006	1598	10		10	15
amide I C=O, C-N, N_H	Parikh & Chorover, 2006	1632-1652	10	9	10	15
v as COOH	Parikh & Chorover, 2006	1720-29	10	9	10	15
C-O	Parikh & Chorover, 2006	1799	10	9	10	15
CO	Müller *et al.*, 2014	2343	10	9	10	15
CO	Müller *et al.*, 2014	2365	10	9	10	15
C-H sym. Stretch CH2	Parikh & Chorover, 2006	2853	10	9	10	15
C-H asym. Stretch CH2	Parikh & Chorover, 2006	2926	10	9	10	15
OH	Madejova & Komadel, 2001	3230-3700	10	9	10	15

For details see Figure 4

cm^{-1}), and the 830 cm^{-1} peak is overlapped by ferrihydrite peaks. Other ferrihydrite bands appear at 930 cm^{-1} and 950 cm^{-1}, whereas the 995 cm^{-1} peak belongs to Si-O stretching of montmorillonite (Madejova & Komadel, 2001). The spectra 5-10 are Ca-pyroxenes with bands 632, 670, 880, 950, 1045 cm^{-1} which belong to Si-O stretching modes (Dyar *et al.*, 2011).

Area 2 is a mixed material of iron oxides (goethite: 675 cm^{-1}, ferrihydrite: 925 cm^{-1}, lepidocrocite: 1150 cm^{-1}) and montmorillonite (625 cm^{-1}, coupled Al-O and Si-O out of plane), 845 cm^{-1} (Al-Mg-OH deformation), 985 cm^{-1} (Si-O stretching), 1100 cm^{-1} (Si-O stretching longitudinal mode), and 3620-3730 O-H stretching modes (Figure 4). The normal montmorillonite has Si-O stretching band at 1003 cm^{-1} (Madejova & Komadel, 2001), which shifted to lower wavenumber. Spectra 1-9 in area 2 contain iron oxides (675, 798, 910 cm^{-1}: goethite – spectra 1-7; 895, 1023, 1150 cm^{-1}: lepidocrocite – spectra 8-9, 692, 910, 3400 cm^{-1}: ferrihydrite – spectrum 10). The Area 2 (spectra 11-15) is pure montmorillonite with bands at 630 cm^{-1} (coupled Al-O and Si-O out of plane), 685 cm^{-1} (Si-O stretching), 835 cm^{-1} (Al-Mg-OH deformation), 875 cm^{-1} (Al-Fe-OH deformation), 915 cm^{-1} (Al-Al-OH deformation), 989 cm^{-1} (Si-O stretching), and 1045 cm^{-1} (Si-O stretching). All spectra of area 2 contain a peak at 720 cm^{-1}, which corresponds to rocking of benzene, and a goethite peak at 675 cm^{-1}.

Both area 1 and 2 contain hydrocarbons, such as C-H aliphatic stretch at 2955 cm^{-1}, 2923 cm^{-1}, 2855 cm^{-1}, C-O-C bend at 1550 cm^{-1}, C-O bend at 1650 cm^{-1}, and O-H stretch in phyllosilicates is also observed in all the measured spectra.

The IR vibrations of isoprenoids were also detected (Parikh & Chorover, 2006; Zhao *et al.*, 2010; Orlov *et al.*, 2012; Chen *et al.*, 2013). According to their investigations, the major vibration of isoprene is centralized near 840, 890, 990 and 1010 cm^{-1}, as observed in area 2.

Some of the major vibrations appear in other IR spectra, such as band 840 cm^{-1}, band 990 cm^{-1}, and 1010 cm^{-1} in area 1. All the IR spectra contain an additional band around 2923 cm^{-1}, which can be related to C-H vibrations of isoprenoids. The IR spectra in area 1 and area 2 contain vibration of PAHs (CN-CH) at 1540 cm^{-1} (amid II) and 1650 cm^{-1} (amid II), C-O vibrations of ketons at 1799 cm^{-1}, 2343 cm^{-1}, 2353 cm^{-1}. The area 1 contain weak OH bands 3230-3700, whereas area 2 contain more intense OH bands near 3650 and 3730 cm^{-1}.

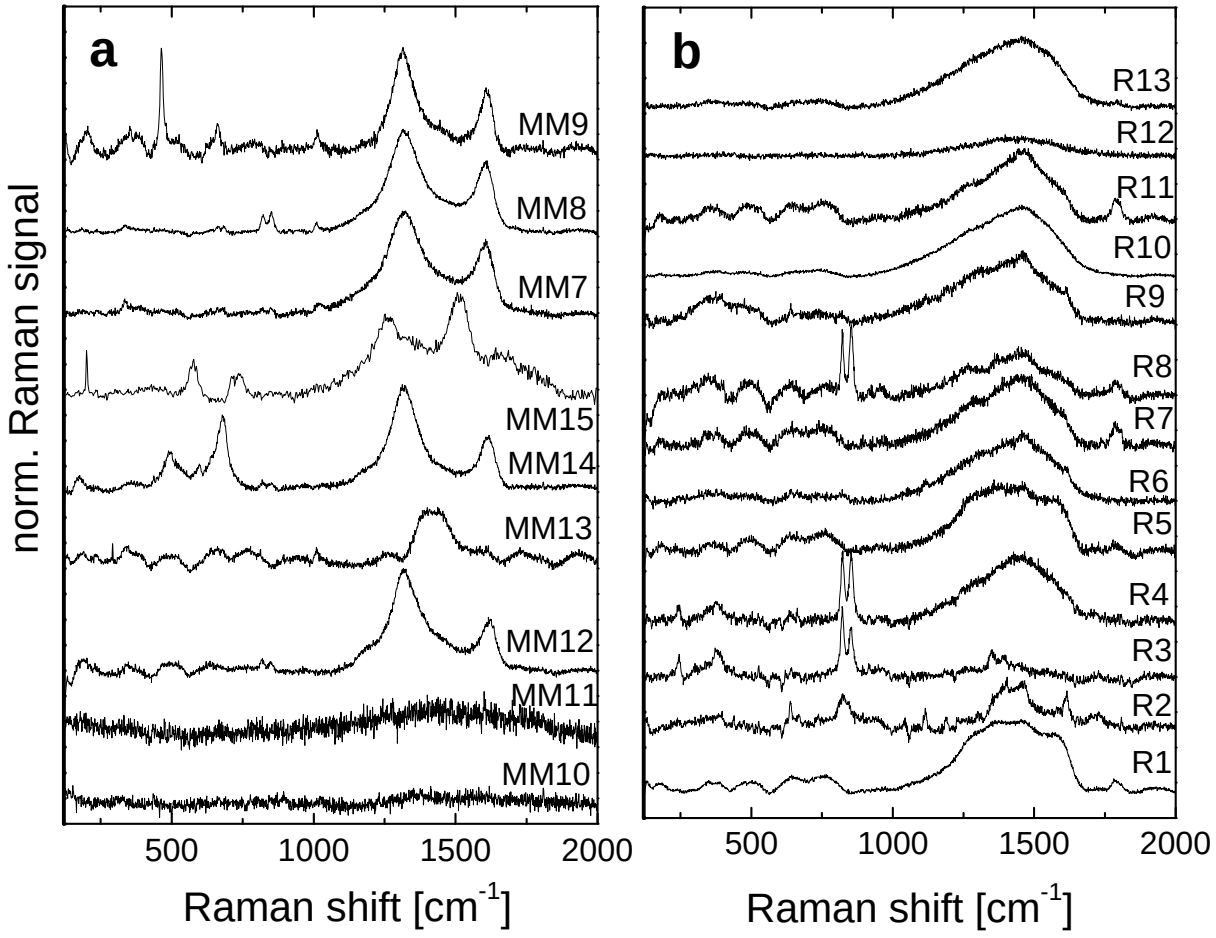

Figure 5. Series of Raman spectra of Mező-Madaras (MM) (a) and Mócs (R) (b) meteorites. MM is dominated by two broad peaks located around 1320 cm^{-1} and 1610 cm^{-1}. These peaks correspond to the so called D and G bands of hydrogenated amorphous carbons, respectively. Mócs is also dominated by a broad feature in the above mentioned region. However, in this case a broad, asymmetric peak can be seen instead of the two well-distinguishable peaks, which can be decomposed into two sub-bands by fitting with Gaussians. The broad peak also corresponds to amorphous carbon, but this phase differs remarkably from that in the MM sample. Decomposition shows the G peak position to be close to 1520 cm^{-1}, a value characteristic for hydrogenated amorphous carbon with sp2 carbon atoms arranged mostly into chains. An additional peak can be seen around 1580 cm^{-1}, corresponding to the sp2 C=C stretching vibrations of aromatic rings. A carbonyl peak can also be observed, which could imply the presence of oxygen in the amorphous carbon structure (SI 4).

4.3 Raman spectroscopy

The Mező-Madaras and Mócs meteorites were investigated by Raman spectroscopy (Table 3, Figure 5, SI 4 - Raman spectroscopy - Mező-Madaras (MM) meteorite). The majority of the spectra recorded in the **Mező-Madaras** sample (MM7–MM9, MM12, MM14, MM15) are dominated by two broad peaks located around 1320 cm^{-1} and 1610 cm^{-1}. These peaks correspond to the so-called D and G bands of hydrogenated amorphous carbons, respectively.

The first is related to the breathing vibrational mode of aromatic rings formed by sp2 carbon atoms, while the second – to the C=C stretching mode of sp^2 C atoms. It should be noted that the Raman spectrum of hydrogenated amorphous carbon usually has a broad feature in the 1000–1800 cm^{-1} region, the shape of which, in addition to the structure, strongly depends also on the excitation wavelength (Tuinstra & Koenig, 1970; Wopenka & Pasteris, 1993; Ferrari & Robertson, 2000; Veres *et al.*, 2006). For 785 nm excitation it consists of bands corresponding to sp2 carbon chains (at 1100–1200 cm^{-1} and 1400–1500 cm^{-1}) and sp^2 carbon rings (breathing mode (D band) in the 1200–1350 cm^{-1}region and stretching mode (G band) 1570 cm^{-1}). In these spectra the position of the G peak is close to that reported for nanocrystalline graphite, indicating the graphitic character of the amorphous carbon phase in the sample. This assignment is supported also by the position and the high (relative to the G peak) intensity of the D band.

Table 3. Distribution of mineral and organic matter composition in Mező-Madaras and Mócs meteorites determined by Raman spectroscopy, estimation of mineral composition on Raman peaks [cm^{-1}]

Mező-Madaras meteorite minerals →	Dickite	Goethite	Ferrihydrite	Lepidocrocite	Montmorillonite	Nontronite	Kaolinite	Olivine	Pyroxene	Quartz	Organic matter	Olivine chemistry (Kuebler *et al.*, 2006)	Pyroxene chemistry (Huang *et al.*, 2000)
MM7											1317, 1607		
MM8	134, 330				186, 681			820, 852	662, 685, 1010		1310, 1605	Fo70	En90Fs10
MM9									353, 660, 1015	121, 205, 464	1312, 1605		En34Fs16Wo50 (1012+3)
MM10	123, 230, 330										1350, 1560		
MM11											1350		
MM12					180, 358, 681			819, 851			1318, 1620	Fo60	
MM13	130, 335, 458								1015		1370, 1400, 1450		En34Fs16Wo50 (1012+3)
MM14						489, 595, 679		820, 851			1320, 1613	Fo70	
MM15			709, 730			280, 670					1260, 1513		
Mócs meteorite													
R1											1354, 1453, 1566, 1780		
R2		123, 390, 635									824 1042, 1116, 1190, 1300, 1395		
R3				247, 372, 529, 641,				821, 853			1354, 1395	Fo78	
R4			709	241, 370, 586, 635,				824, 854			1428	Fo100	
R5							356, 472, 635, 747				1358, 1457, 1580, 1778		
R6											1453, 1603		
R7							355, 478, 630, 745				1284, 1787		
R8	128, 335						355, 472, 630, 743	819, 849				Fo62	
R9							345, 639, 742				1312, 1453, 1609		
R10		129, 639	736								1560, 1780		
R11							176, 350, 477, 635, 745				1250, 1444		
R12		127, 630									1400		
R13			349, 739				350, 476, 635, 745				1444, 1790		

Many of the spectra of the **Mócs** sample (R1, R4–R11, R13) are also dominated by a broad feature in the abovementioned region. However, in this case a broad, asymmetric peak can be seen instead of the two well-distinguishable peaks, which can be decomposed into two sub-bands by fitting with Gaussians. The broad peak also corresponds to amorphous carbon, but this phase differs remarkably from that in the MM sample. In the R4, R6, R9, R11, and R13 spectra the maximum of the broad band is around 1460 cm^{-1}. Decomposition shows the G peak position to be close to 1520 cm^{-1}, a value characteristic for hydrogenated amorphous carbon with sp2 carbon atoms arranged mostly into chains. This conclusion is also supported by the relatively low intensity of the D band, related to breathing vibrations of aromatic rings. In the R1 and R5 spectra (and to some extent in the R7–R9 and R11), however, an additional, well-distinguishable peak can be seen around 1580 cm^{-1}, corresponding to the sp2 C=C stretching vibrations of aromatic rings (Mapelli *et al.*, 1999). Its presence, together with the higher scattering intensity in the D band region, indicates the higher amount of aromatic rings in the hydrogenated amorphous carbon phase. A carbonyl peak can also be observed in the R1, R5, R7, R8, and R11 spectra in the 1700–1800 cm^{-1} region that could imply the presence of oxygen in the amorphous carbon structure (Veres *et al.*, 2006).

Hydrocarbon peaks appear between 1000 and 1600 cm^{-1}, overlapped by the broad feature of amorphous carbon in the majority of these spectra. The peaks found at 1300 cm^{-1} (MM8–9, MM12, MM14, R2 spectra), 1400 cm^{-1} (MM13, R2, R3 spectra) and 1450 cm^{-1} (R1, R2, R6, R9, R11, R13 spectra) probably correspond to vibrations of different CH_2 and CH_3 groups. They are in good correlation with peaks of CH_3 and CH_2 groups observed at 1296 cm^{-1}, 1335 cm^{-1}, and 1441 cm^{-1} (Mapelli *et al.*, 1999) in the iron-oxidizing bacterial mat at the rim of ooids in Sturtian oolitic sandstone (Gyollai *et al.*, 2014). Other peaks, related to organic materials of recent iron bacteria (Parikh & Chorover, 2006) can also be detected around 1454–1482 cm^{-1} (CH2 vibration, R1–2, R5–7, R9 spectra), 1360–1450 cm^{-1} (COO-vibration, R1–2, R4, R6–7 ,R11–13 spectra), 1220–1260 cm^{-1} (isoprenoid PO2- vibration, MM5, R11 spectra), 1170 cm^{-1} (C-O vibration), 1114–1118 cm^{-1} (isoprenoid C-O-P, P-O-P vibration, R2 spectrum), 1042–1046 cm^{-1} (PO32 vibration, R2 spectrum), 1039–1043 cm^{-1} (P-OH P-OFe vibration, R2 spectrum), 1016–1020 cm^{-1} (P-OFe ring vibrations, MM9 spectrum) and 1016–1020 cm^{-1} (P-OFe vibration, MM9 spectrum). The presence of isoprenoids, characteristic of prokaryota membranes, was supported by FTIR-ATR spectroscopy too (Srinivasan, 1935; Igisu *et al.*, 2009).

The kandite group of minerals (kaolinite, dickite, halloysite), the peaks of which appear in several measurement points (MM8, 10, 13, R2, R4, R5, R7–12), correspond to weathering of Fe-Mg-silicates (Frost, 1995). Our spectra contain O-Al-O (131 cm^{-1} for dickite) and O-Si-O (120 cm^{-1} for dickite, 127 cm^{-1} for kaolinite) symmetric stretching, Si-O band (340 cm^{-1} for dickite), Si-O-Si stretching (744 cm^{-1} for halloysite, 752 cm^{-1} for kaolinite).

The pyroxene (662, 685, 1010 cm^{-1}) occur in MM8, MM9, MM13. Mineral endmember composition can be estimated using Huang *et al.* (2000) calibration: En90Fs10 (MM8), En34Fs16Wo50 (MM9, MM13) (Table 3). The olivine doublet (820, 850) appears in the spectra taken in the MM8, MM12, MM14, R3-4, and R8 points. The olivine is weathered, and the only major bands appear near 820 cm^{-1} and 850 cm^{-1}. The composition of olivine can be estimated using calibration of Kuebler *et al.* (2006), which varies between Fo60 (MM12) and Fo70 (MM8, MM14).

The smectite group of minerals has been found in many measurement points (MM8, MM12, MM14-15, R2, R4-5, R7-13), and their formation is driven by syngenetic activity and/or diagenesis of iron-oxidizing bacteria and weathering of olivine. Structural lattice modes of montmorillonite minerals (Bishop & Murad, 2004) appear at 186, 205, 170, 476, 570, 635, and 709 cm^{-1}. Nontronite peaks can be seen in the MM14-MM15 spectra (489, 595, 679 cm^{-1}). Al-O-Si, Si-O lattice bands are centered at 495, 593, and 678 cm^{-1}, Fe-Fe-OH vibration at 822 cm^{-1} for nontronite (Hradil *et al.*, 2004). The montmorillonite marks oxidizing, while the nontronite marks reducing condition during the diagenesis of FeOB filaments.

The spectra also contain iron oxide phases, like ferrihydrite (MM15, R10, R13), lepidocrocite (R3-4), and goethite (R2, 10, 12). The presence of iron oxides marks the rate of diagenetic alteration of FeOB filaments (Parikh & Chorover, 2006; Watanabe *et al.*, 2008). Spectrum MM9 contain bands of quartz (205, 464 cm^{-1}).

5 Discussion

Overview of UOC alteration studies and the open questions and contradictions arose in several measurements are summarized in SI. 1A (General main interpretations/conclusions, questions and contradictions (A) concerning UOC based on selected references and the proposed interpretation and answers based on recent study (B)).

Our answers based on studies on L and LL chondrites are summarized in SI. 1B (General main interpretations/conclusions, questions and contradictions (A) concerning UOC based on selected references and the proposed interpretation and answers based on recent study

(B)), which includes the recognition and acceptance of Fe-rich filamentous mineralized biotextures (MMPT) identified by optical microscopy with suitable magnification, which was followed by the IR and Raman measurements of mineral products and organic compounds in the vicinity of the observed MMPT objects. Presence of quartz is unusual in chondritic meteorites, it can be explained by mineralization of EPS of FeOB, in which process silica segregated similarly to terrestrial analogues (Peng *et al.*, 2007).

The broadened bands of iron oxides, and shifting of bands to lower wavenumbers of montmorillonite, can be explained by biogenic processes (Markovski *et al.*, 2017). The band 1012 cm^{-1} of Ca-pyroxenes shifted to higher wavenumber, due to distortion of SiO_4 tetrahedra. The biomediation could cause distortion of original crystal structure (Markovski *et al.*, 2017).

5.1 Interpretations

Interpretation 1: Data confirm dense and invasive terrestrial microbially mediated contamination in the chondrites, supported by microtexture, micromineralogy and embedded organic compounds, which affected most of the mass of the samples. However, the appearance of the products of the 3 classical (thermal, aqueous and impact) transformation processes have been manifested in microbially mediated texture. This arises a contradiction: how could it be that all these classical transformations have been occurred to happen on the parent bodies, while the microbial processes happened separately, in terrestrial conditions, although the MMTP had interwoven all the textural and mineralogical assemblage. This contradiction can be solved by:

Interpretation 2: Based on terrestrial analogies, microbial mediation is a sudden process comparing to geological times, very ancient, widespread and occur in various (extreme) environments under determined conditions. It can consume previous and also produce new minerals, if the chemical compounds (Fe, etc), wet conditions, Eh and pH are favourable. After formation, MMPT and the embedded minerals and organic material can survive billions of years proposing occurrence on parent bodies.

Regardless of geological age and geographical location, the Fe-rich structures associated with microbes and paleoenvironments always bear witness to gradients of oxygen and Fe^{2+} along various mineral interfaces (Préat *et al.*, 2000; Konhauser *et al.*, 2002). Bacterial cells can precipitate a wide variety of Fe minerals through various metabolic processes (Konhauser *et al.*, 1998). No intact and convincing microbial fossils have yet been identified even in Fe-rich biomats similar to banded iron formations (BIFs) (Konhauser *et al.*, 2002), which give rise to biogenicity problems. Consequently, any attempt to prove a direct microbial role in Fe biomineralization must rely on circumstantial evidence. Therefore, after the first step of morphology observation, the second one is the identification of minerals: the mineralized biosignatures, which have a greater chance of surviving over geological time if they are rapidly and extensively encrusted (like goethite after microbially produced ferrihydrite). Therefore morphology in combination with mineralogy and chemistry bioindicators makes complex interpretation possible (Baele *et al.*, 2008).

In our work the first step was the recognition and acceptance of Fe-rich filamentous biotextures (MMPT). Based on microbial signatures in Fe-rich brown haloes in the chondrites, we focused on Fe(II) oxidizing microbial activity (Figure 2). Suitably high magnification OM shows filamentous microbial-like morphology with pearl necklace-like inner signatures deeply and extensively embedded in the stone meteorites, together with a bubble-like invasion front (consisting of a similar filamentous morphology) towards a broken chondrule (Figure 2).

The second step, the *in situ* mineralogical studies, proved the presence of Fe biominerals, ferrihydrite, lepidocrocite, goethite and magnetite similar to terrestrial occurrences (Fortin *et al.*, 1997; Konhauser *et al.*, 1998; Ehrlich *et al.*, 2002), confirming biogenicity, which was supported also by variable organic matter constituents occurring in the microbial-like textures as remnants of earlier microbial activity, also embedded in the stone meteorites (Figure 4-5).

Such indicators are only partly detectable in chondrites, because of the unique conditions of their formation. The most prominent candidates for Fe-bearing mineral bioweathering and biomineralization are prokaryotes (Konhauser *et al.*, 1998; Ehrlich *et al.*, 2002). So, we propose mineralizing prokaryotes as better candidates to prove microbial mediation, *e.g.* Fe-bacteria causing Fe-oxide biomineralization and characteristic filamentous microstructure, together with organic matter combined with them. Light $\delta^{13}C$ can also raise microbial mediation similar to recent and ancient terrestrial occurrences (Table 1) (Fortin *et al.*, 1997; Polgári *et al.*, 2012).

On the other hand – based on stable C isotope studies made on bulk samples – strongly decreased $\delta^{13}C$ data (–27‰ or less) were also reported (Grady *et al.*, 1982), and interpreted as an effect of terrestrial contamination (based on selective enrichment of ^{12}C by living organisms), but T selective measurements did not support that scenario (Greenwood & Franchi, 2004). Concerning terrestrial contamination (Kerridge, 1985), the possibility of contamination was discounted, there being no obvious correlation with carbon content, arguing that the spread of results reflects intrinsic

sample inhomogeneity. The trend of decreasing $\delta^{13}C$ values was interpreted as a consequence of increasing metamorphic grades (Greenwood & Franchi, 2004).

Our model concerning chondritic diagenesis of microbial mineralization as a gradually increasing possible cofactor in the alteration of texture fits these data well. Therefore, in our model, the gradual fading of the rims of chondrules – mainly in the case of the UOCs – is a *consequence of not (only) thermal metamorphism but of the microbially mediated transforming effects*.

In general, there are no specific signatures for kerogens in their Raman spectra that can be used to distinguish between them and hydrogenated amorphous carbon (while the opposite is not true – some types of hydrogenated amorphous carbon can easily be distinguished from kerogen by their Raman spectra). Such signatures are not expected to exist, since kerogen and graphitic hydrogenated amorphous carbon have a very similar structure (especially in terms of structural units contributing to their Raman spectra). Kerogen is a generalized term used for organic chemical compounds found in rocks, whose main constituents are hydrocarbons. Hydrogenated amorphous carbon is a disordered material consisting of carbon and hydrogen. The Raman spectra of both are dominated by the so-called disorder-related (D) and graphite-like (G) bands, originating from breathing vibrations of sp^2 hybridized carbon rings and stretching vibrations of sp^2 C-C bonds for both materials.

Because of the high level of polycondensation of hydrocarbons, the D and G bands of kerogen are located between 1310–1360 cm^{-1} and 1580-1600 cm^{-1}, respectively (Kelemen & Fang, 2001; Du *et al.*, 2014). These peak positions are characteristic also of graphitic hydrogenated amorphous carbon and these features can be seen in the MM7-MM9, MM12 and MM14 spectra of our Mező-Madaras meteorite sample. On the other hand, the R1, R4-R7, R9-R11 and R13 spectra of the Mócs meteorite have a broad band in the 1000 - 1700 cm^{-1} wavenumber region, without well-distinguishable D and G peaks. This feature is characteristic of hydrogenated amorphous carbons with a high amount of sp^2 hydrocarbon chains (Veres *et al.*, 2006) and this kind of spectrum has not been reported for kerogens in the literature, which indicates that the carbon material observed in the sample is not kerogen.

The presence of olivine and pyroxene shows the original Fe-Mg-silicate composition, and the montmorillonite and kandite clays of the spectra are proof of weathering of olivine, while the appearance of ferrihydrite corresponds to microbial originated remobilization of Fe from Fe-rich Fe-Mg-silicates and troilite.

Two authigenic clay formation types were detected in our chondrites, which offer a chronological diagenetic interpretation; (i) smectite group, and (ii) kandite group. The smectite group minerals are generally reported as alteration products in weathering zones of slightly basic, suboxic conditions, often containing a considerable amount of Fe (montmorillonite, nontronite). The kandite group minerals (dickite, halloysite, kaolinite) are important alteration indicators of aluminosilicate minerals (in weathering zones, in hydrothermal systems and igneous rocks, especially glassy basaltic rocks), often found in close association with goethite and limonite (Kerr, 1952). In our case, microbial weathering could be responsible for this first step (1). As a second step (2), vermiform kandites formation (from remnants of aluminosilicate minerals) reflects a change from pore-fluid chemistry to more acidic conditions and positive Eh, which may have resulted from *in situ* bacterial processes via "aerobic" (minerals having a great amount of oxygen) bacterial oxidation of organic matter (Curtis, 1977). As a third step (3), later anaerobic microbial processes raised pH (becoming alkaline) but lowered Eh, resulting in the formation of montmorillonite and nontronite. Montmorillonite is a common diagenetic product of microbial Fe oxi-hydroxides and the segregating SiO_4 polymers mobilization via silicate alteration that is also common in terrestrial environments (Cole & Shaw, 1983; Fisk *et al.*, 2006). Diagenetic products of the activity of Fe-oxidizing microbes (also EPS mineralization) in the form of goethite and green clays, montmorillonite and nontronite are present as very characteristic constituents in all the studied chondrites. Abiogenic clay formation as an alternative process could also contribute to their formation.

5.2 Clay formation

Besides alteration of previously formed silicates, direct hydrothermal and also microbially mediated clay mineral formation also proposed by the literature (Juniper & Fouquet, 1988). This microbially mediated clay mineral precipitation is most probably microbially induced mineralization, where the microbes behave as template for mineralization, but in the vicinity of hydrothermal discharge systems, *e.g.* formation of nontronite can be formed on the cell or EPS surface via a more active process (Köhler *et al.*, 1994). Konhauser & Urrutia (1999) proposed also a formation model for authigenic clay mineral formation. After death of cells the decomposition of cells and EPS starts and ions, which bound on their surface, will liberalize and a complex transforming mineralization starts which can result clay mineral formation, mixed carbonates, feldspar, silica, apatite, etc.,

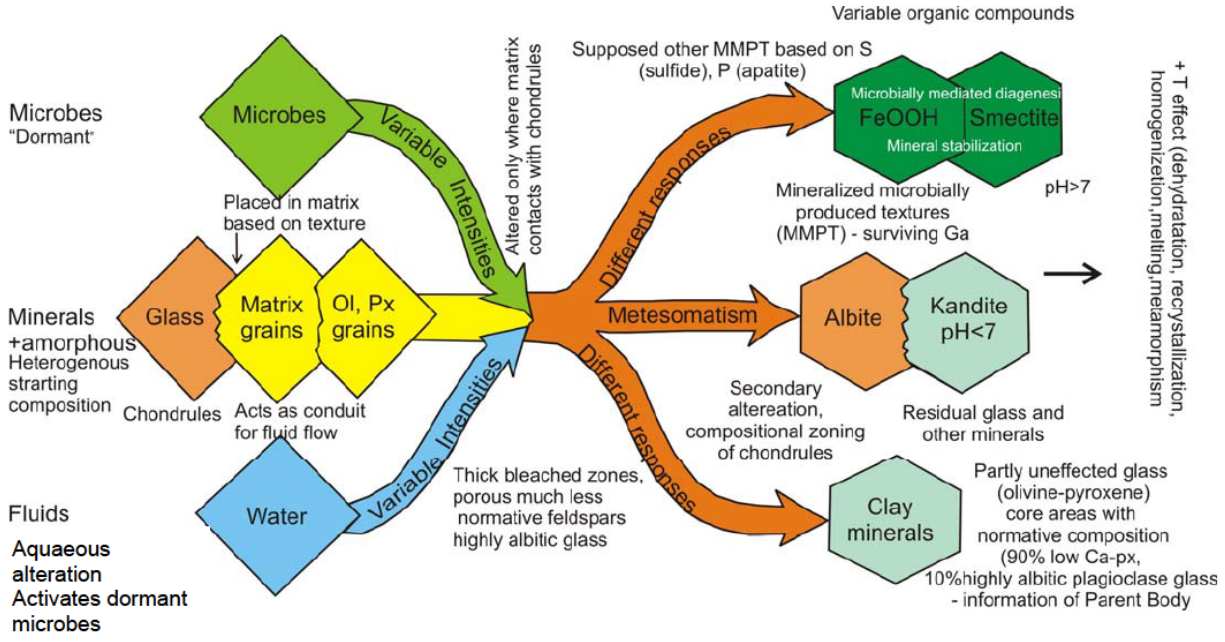

Figure 6. Summary of the mineral transformations if three threads of actors are individually considered in the complex system of the UOC alteration processes: water (fluids), initial minerals and microbes. Heterogenity at all stages, variable mass ratio conditions and intensity of processes on parent body abiogenic and microbial processes are together in variable ratios. Legend: Ol - olivine; Px - pyroxene.

depending on the geochemical conditions. These poorly crystallized minerals can form more stable minerals on time (Konhauser *et al.*, 1998; Dupraz & Visscher, 2005).

Clay formation, that caused the homogenization of chondrules and minerals as well as matrix, has also been observed for Semarkona and Bishunpur LL3.0 chondrites (Hutchison *et al.*, 1987). This process offers an alternative explanation for the gradual transformation of diffusional fading of the chondrule rims during the increasing metamorphism for L3–6 chondrites. Observations of the clay minerals in asteroid spectra refer to the possibility of the occurrence of montmorillonite also in other chondritic parent bodies (Ostrowski *et al.*, 2011). Clay minerals (O-H stretching bands) in the studied chondrites also offer T estimation based on mineral stability of less than 400°C. Based on different estimation methods, various T maximum conditions were proposed for UOC (Huss *et al.*, 2006). Our data fit well with the lower T values.

Consequently, it is concluded that the MMPT can be interpreted as representing filamentous prokaryotes that invaded the chondritic texture in aquatic conditions syngenetically (no modern terrestrial contaminants), that grew, woven and died in aquatic regimes on the parent body of the chondritic meteorites, before they entered the Earth's atmosphere (Figure 6, SI 5 - Detailed mineral alteration pathways).

5.3 Biogenicity aspects

Based on the above results, concerning aspects of biogenicity established and proposed as complex merits in terrestrial geological samples by Cady *et al.* (2003), convincing similarity occurs on four hierarchical levels Bérczi (2018) on (1) atomic level, (2) molecular level, (3) mineralogical level and (4) microtextural level, and the following can be stated:

(i) micro-textural features ("microbial microtexture" – filamentous, coccoid-like, vermiform, etc.) – occur;
(ii) "bioindicator" minerals and mineral assemblages – occur;
(iii) embedded variable organic matter – occur;
(iv) signs of "vital effect" – isotope signals – occur;
(v) recent analogies on microbially mediated mineralization (terrestrial) – occur;
(vi) preservation – occur; and only
(vii) *environmental analogies (sedimentary, etc.) cannot be interpreted* in the recently studied meteorites. We detected also similar results concerning Kaba meteorite (Polgári *et al.*, 2018).

5.4 Terrestrial contamination

Terrestrial contamination cannot be excluded, but is not responsible for MMPT formation in chondrites, because (i) textural evidence does not support contamination tendencies from the samples' marginal parts towards inner parts, (ii) MMPT is deeply embedded in the thin sections of stone meteorite and not on their surface, (iii) 70–80% of the thin sections are affected by MMPT in a nano-scale unseparable form, and (iv) the studied meteorites were stored in dry museum conditions, which should prevent them.

5.5 The age considerations

The age of these chondrites is 4.55 Ga. The age of the observed microbial signatures (morphology, Fe biominerals, organic matter remnants and clay formation) is comparable to ancient (ca. 3 Ga) and modern terrestrial occurrences (Schopf *et al.*, 2007). Both sets of data prove that these mineralized microbial signatures could be preserved over geological time. In our case, a new aspect based on MMPT (OM) was used to prove microbial mediation instead of simply organic compounds. On the other hand, organic compounds combined with MMPT especially confirm microbial mediation.

If the scenario that the opaque fine-grained matrix was accumulated onto the chondrules and mineral grains from the solar nebula and remnants of the interstellar cloud is valid, and the invasion appears to start from the matrix toward the chondrules and minerals (microtextural evidence), then this supports the hypothesis that microbial life existed in the interstellar cloud at the time the Solar System formed. This observation attaches an independent line of events to the evolution of the chondritic parent body and implies a revision of the models explaining the origin of life on Earth.

5.6 Perspectives and broader implications

MMPT in the form of pearl necklace-like, vermiform inner signatures, embedded in the stone meteorites has been observed for the first time in thin sections of chondrite from suitably higher magnifications by OM. IR and Raman measurements confirmed the OM observations as the products of the advancing primordial syngenetic microbial process.

In the chondritic textures we observed that microbial "invasion" started in the fine-grained matrix and extended into the chondrules mainly through the Fe-containing minerals. The MMPT is very extensive, reaches 70-80% of the sections, and is intimately woven in the full cross-section of the thin sections of the whole stone meteorite.

Earlier analyses resulted in several possible interpretations of UOC evolution but no satisfactory conclusion on pathways has been reached. Our proposed simplified order of processes and important influencing factors are as follows: We consider that various UOC and OC samples probably represent systems which were "frozen" at different stages of evolution/development, depending on → the effect of mass balance ratios (how much of this or that "component" existed) → the quantity of much more amorphous material than water + microbes → via crystallization the effect ends if there is no supply of water and chemical nutrients. The "frozen" effect can happen at various stages. The studied UOC and OC samples may represent the very different transition phases (Table 4).

From the observed microtextural facts and IR and Raman spectroscopy measurements, the following more detailed and coherent comparative interpretations were elaborated.

5.7 Time sequence of the alteration types

According to the velocity of particular processes, we can try to reconstruct a time sequence of the various types (SI. 6 - Theoretical chronological prediction of the tendency of the M-W-T processes):

1. microbial mediation – this is dependent on water, ions and raw material, and the binding energy of grains (glass, matrix, larger-minerals)
2. aqueous alteration – dependent on the quantity of water and the ions dissolved in it,
3. dehydration – dependent on temperature
4. thermal metamorphism – diffusion, dependent on temperature.

On the basis of this time sequence, the alteration might have been started by the microbial invasion coming from the fine-grained matrix under aquatic conditions and quickly spread to the glasses in the mesostasis of the chondrules, and finally extended into the larger mineral grains of the chondrules, mainly through the Fe-containing minerals (based on the recent results). The microbially mediated alterations caused microbial weathering and biomineralization, represented by surviving albite (replacement of glasses), phyllosilicates (clay minerals) in the matrix and at the white bleached areas and at the chondrule rims. The sequence of these products depends on the early complex behavior of bleaching.

Table 4. Simplified order of processes and important influencing factors.

Heterogeneous start (variable minerals and amorphous phases)	+	Variable rate of aqueous, temperature and microbial mediation by variable intensity (microbial weathering-leaching, biomineralization, EPS mineralization) (This is our recent proposal)	+	Mass balance aspects, how many from this and that component (mineral, amorphous and water, etc.)	+	Different responses	+	Time effect of ending "Frozen"	For investigators these facts seem hardly interpretable according to the present nomenclature and known (canonic) processes.

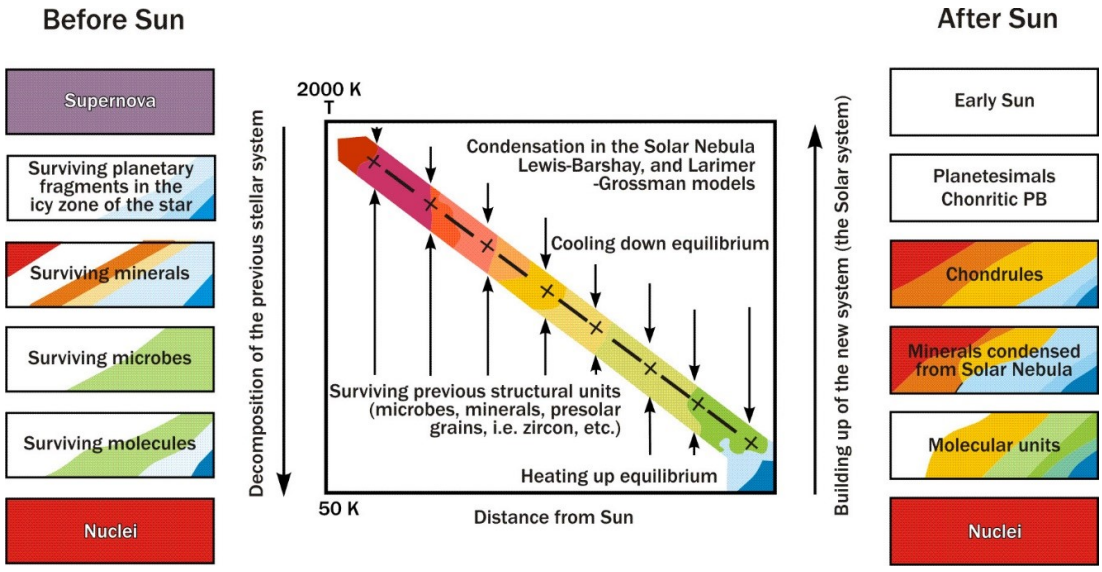

Figure 7. Proposed condensation-evaporation "hysteresis" range in the primordial Solar System. Condensation (after Sun objects, right coloumn) and evaporation (previous objects surviving the formation of the Sun, left coloumn) in a hierarchical sequence, top larger, bottom smaller. Legend of colors: violet- supernova; red - high temperature (refractory) minerals; orange - dry rock-forming minerals; yellow - hydrated silicates; green - microbes; light blue and dark blue - ices; dark red at bottom - nuclei (isotopes).

Parallel to the microbially mediated processes, water (or fluid) abiogenic processes may also produce phyllosilicates, although other types. Dehydration and thermal metamorphism by diffusion are strongly dependent on temperature, so these are the last, gradually increasing transformation types.

Where is the gap in which the microbes could participate in the processes of the early Solar System? The models interpret the materials "after Sun" in terms of condensation, and "before Sun" through the surviving primordial (as presolar grains) materials. The two material subsystems leave a gap for hysteresis (Figure 7). Most of the structures in the hierarchy of the supernova previous to the Sun are destroyed, but cooler regions might have been able to preserve these contaminants for the "after Sun" period components. The survival and decomposition of structures are locally heat-dependent. The surviving microbial contaminants may have been transported into the central Solar System also by comets.

5.8 Parallel origin of organic compound formation

Organic compounds could have been an important source of the prebiotic compounds required for the origin of life on Earth or elsewhere. Extraterrestrial amino acids, contents of CH and CB have been reported in carbonaceous chondrites (Burton *et al.*, 2013). Amino acids were found in other ordinary and carbonaceous chondrites by Chan *et al.* (2012), but they proposed extraterrestrial origin, and the formation due to gas-grain reaction after cooling at lower temperature of the parent body. Organic material was found in microbial-like FeOB meshwork, which affected up to 70-80% of the samples (this study). If this is terrestrial contamination, the alteration of meteorites could not be studied as parent body processes (Gyollai *et al.*, 2017; Polgári *et al.*, 2017). Burton *et al.* (2011) pointed out, that presence of water, aqueous alteration is important for formation of amino acids in solar nebula. For activation of dormant spores of bacteria

Table 5. Summary of hierarchy of the novel results and interpretations.

Initial condition: Detailed geochemical and mineralogical studies for decades without coherent interpretation for UOC over thermal metamorphism and aqueous metasomatism Suggested reason: missing of textural study on adequate magnification by adequate method and interpretation based on multilevel structural hierarchy of materials (component - texture - process)		
↓		
New tool: Optical Rock Microscopy (OM) on adequate magnification Based on experiences (Polgári *et al.*, 2012)		Origin of ancient microbial life based on MMPT as new aspect (preserved minerals and/or pseudomorphs forming microbial texture as evidence of ancient microbial mediation)
↓		Syngenetic deep microbial mediation on parent body
Triggering first observation of mineralized microbially produced textures (MMPT) as brownish filamentous necklace-like (vermiform) textures as basic features in micrometer dimension	→	MMPT can survive thousands of millions of years
↑		The observed textural features exclude recent terrestrial contamination Offers new (3.) model for chondrite transformation and alteration as syngenetic microbial mediation running parallel with the earlier known thermal and aqueous alterations
Confirmation supported by in situ high resolution investigations by FTIR and RAMAN on representative parts offering adequate number of data for interpretation: - brown color raises Fe-oxidizing bacteria in filaments formation - biominerals (Fe-oxides and hydroxides, clay formation as diagenetic product) - variable organic compounds - $\delta^{13}C$ (−22‰) (isotope signal)		Offers alternative model for T metamorphism as: Diagenetic products (clay minerals) of microbially mediated mineralization, becoming more and more intense from L3 to L6 similarly to Earth analogues; L3 to L6 show more and more intense clay content showing a more and more difficult transparency seemed to be homogenization effect T estimation based on clay mineral stability (O-H streching bands) is less than 400°C. Key to coherent interpretation of present data

the presence of water on planetary body is also necessary (Jones & Lineweaver, 2010). Extraterrestrial abiogenic and microbial organic compound formation processes might have existed side by side.

The MMPT gives a new aspect to the study of chondrite processes on the parent body and the evaluation of past microbial life instead of organic compound based proposals, and raises the parallel origin of organic compound formation of abiogenic and microbially mediated types.

6 Conclusion

In this work we offered two interpretations on micro textural, mineralogical and organic matter distribution results in chondrites. Also we applied a new method for microbial fossil identification in chondritic meteorites. This method was based on the recognition of the MMPT in the chondritic texture (Table 5; SI. 1 - General main interpretations/conclusions, questions and contradictions (A) concerning UOC based on selected references and the proposed interpretation and answers based on recent study (B)).

Interpretation No. 1

Data confirm dense and invasive terrestrial microbially mediated contamination in the chondrites, supported by microtexture, micromineralogy and embedded organic compounds, which affected most of the mass (up to 80%) of the samples. However, the appearance of the products of the 3 classical (thermal, aqueous and impact) transformation processes have been manifested in microbially mediated texture. This arises a contradiction: how could it be that

all these classical transformations have been occurred to happen on the parent bodies, while the microbial processes happened separately, in terrestrial conditions, although the MMTP had interwoven all the textural and mineralogical assemblage.

Interpretation No. 2

1. The MMPT and the embedded minerals and organic matter give a new aspect to the study of chondrite processes on the parent body and the evaluation of past microbial life, instead of organic compound based proposals, and raises the parallel origin of the organic compound formation of abiogenic and microbially mediated types in the Solar System.
2. The MMPT is a valuable source of information about the origin of past microbial life based on the preserved minerals and/or pseudomorphs which were formed by microbial interactions in the texture by the primordial syngenetic microbial mediation. Further, the organic compound dataset also confirmed this scenario, together with negative $\delta^{13}C$ values.
3. The MMPT can be preserved for thousands of millions of years, as also observed in terrestrial samples.
4. The MMPT excludes recent terrestrial contamination as a main process.
5. The interpretation of our measurements and systematics is key to a coherent interpretation of the long-debated and thought dataset collected on chondritic alterations, offering the proposed simplified order of processes and important influencing factors: UOCs and OCs probably represent systems in a sequence which were "frozen" at different stages of development.
6. The three-thread process-description (A-M-T) offers a more plausible model for the increasing T metamorphism running parallel with it.
7. The interpretation of the syngenetic and/or diagenetic products (clay minerals) of microbially mediated mineralization is in accordance with Earth analogues. If a water supply exists, it becomes more and more intense from L3 to L6, giving more and more intense clay content (the gradual increase of the obscuring transparency seems to be a homogenization effect).
8. The MMPT model also gives a T estimation based on clay mineral stability (O-H stretching bands) that is less than 400°C.

Our study (1) contributes to the extension of bioweathering and biomineralization studies over a wide range of UOCs and OCs, (2) offers an alternative model for the homogenization of chondrules by microbial weathering and diagenesis, suggesting that primitive microbial constituents also contributed to the formation of the early planetary accretion, and (3) helps to elucidate the suggestion that the formation of life in the Solar System began to develop from not the molecular but the microbial level, and (4) initiates research on various occurrences of microbes not only on Earth but in any extremal environments in the Solar System, and (5) proposes that the "microbially contaminated dust" (with dormant microbes) is probably continuously streaming from presolar objects even today.

Acknowledgment: The authors thank the support of National Research, Development and Innovation Office, National Scientific Research Found No. 125060, Support of Excellence of Research Centre for Astronomy and Geosciences, Institute for Geological and Geochemical Researchand Hungarian Academy of Sciences. Comments of anonym reviewers are highly appreciated.

References

Baele, J. M., Bouvain, F., De Jong, J., Matielli, N., Papier, S., & Préat, A. 2008, In: Instruments, Methods, and Missions for Astrobiology XI (Vol. 7097, p. 70970N 12p.). International Society for Optics and Photonics.

Bérczi, Sz. 2018, In: Nagy M. & McIntosh R. (Eds.), Comprehensive Research on Kaba Meteorite, Acta GGM Debrecina Geology, Geomorphology, Physical Geography Series, Debrecen University Press, Special Issue, 31-53.

Bishop, J. L. & Murad, E. 2004, J. of Raman Spect., 35 (6), 480-486.

Brearley, A.J. 1997, In: Zolensky M., Krot A., & Scott E. R. D. (Eds.), Workshop on Parent-Body and Nebular Modification of Chondritic Materials, 4027, LPI, Houston.

Burton, A. S., Elsila, J. E., Hein, J. E., Glavin, D. P., & Dworkin, J. P. 2013, Met & Planet Sci. 48 (3), 390-402.

Burton, A.S., Glavin, D.P., Callahan, M.P., Dworkin, J.P., Jenniskens, P., Shaddad, M.H. 2011, Met. & Planet. Sci., 46(11), 1703-1712.

Cady, S.L., Farmer, J.D., Grotzinger, J,P., Schopf, J.W., & Steele, A. 2003, Astrobiol., 3 (2), 351-369.

Chan, H. S., Martins, Z., & Sephton, M. A. 2012, Met. & Planet. Sci., 47(9), 1502-1516.

Chen, D., Shao, H., Yao, W., & Huang, B. 2013, Internat. J. Polymer. Sci., Article ID 937284, http://dx.doi.org/10.1155/2013/937284.

Claus, G. & Nagy, B. 1961, Nature, 192, 594-596.

Cole, T. G. & Shaw, H. F. 1983, Clay Miner., 18, 239-252.

Curtis, C. D. 1977, Philos Trans Royal Soc Lond, A (Mathemathical, Physical, and Engeering Sciences) A286, 353-371.

Du, J., Geng, A., Liao, Z., & Cheng, B. 2014, J. Anal. Appl. Pyrol., 107, 242-249.
Dupraz, C. & Visscher, P.T. 2005, Tends Microbiol., 13, 429-438.
Dyar, M. D., Glotch, T. D., Lane, M. D., Wopenka, B., Tucker, J. M., Seaman, S. J. et al. 2011, Polar Science, 4(4), 530-549.
Ehrlich, H.L. 2002, Geomicrobiology (4th edition), Marcell Dekker Inc., 183 – 274.
Engel, M. H. & Nagy, B. 1982, Nature 296, 837-840.
Ferrari, A. C., & Robertson, J. 2000, Physical Rev. B, 61(20), 14095.
Fisk, M. R., Popa, R., Mason, O. U., Storrie-Lombardi, M. C., & Vicenzi, E. P. 2006, Astrobiol., 6(1), 48-69.
Fortin, D., Ferris, F. G., & Beveridge, T. J. 1997, In: Banfield J. & Nealson K.H. (Eds.), Geomicrobiology: Interactions between microbes and minerals, Mineralogical Society of America, Reviews in Mineralogy 35, 162–180.
Frost, R. L. 1995, Clays & Clay Miner., 43(2), 191-195.
Glotch, T. D. & Rossman, G. R. 2009, Icarus, 204, 663–671.
Grady, M. M., Swart, P. K., & Pillinger, C. T. 1982, XIII Lunar & Planet. Sci. Conf. (LPI, Houston), 277-278.
Graham, A. L., Bewan, L., & Hutchison, A. W. R. 1985, Catalogue of meteorites. British Museum (NH), London.
Greenwood, R. C. & Franchi, I. A. 2004, Met. & Planet. Sci., 39(11), 1823-1830.
Grossman, J. N., Alexander, C. M. O., & Wang, J. 1997, In: Zolensky M., Krot A., & Scott E. R. D. (Eds.), Workshop on Parent-Body and Nebular Modification of Chondritic Materials (17-19 July 1997, Maui, Hawai'i, USA), LPI Technical Report, LPITR 97-02, Houston, TX: Lunar and Planetary Institute,19.
Grossman, J. N., Alexander, C. M. O., Wang, J., & Brearley, A.J. 2000, Met. & Planet. Sci., 35(3), 467-486.
Grossman, J. N. & Brearley, A. J. 2005, Met. & Planet. Sci., 40, 87-122.
Gyollai, I., Polgári, M., Veres, M., Nagy, S., Popp, F., Mader, D. et al. 2014, Comm. Nam. Geol. Surv. 15, 117-133.
Gyollai, I., Polgári, M., Bérczi, S., Veres, M., Gucsik, A., & Pál-Molnár, E. 2017, Workshop on Chondrules and the Protoplanetary Disk (27-28 February 2017, London, United Kingdom), LPI Contributions no. 1963, id. 2005.
Hamilton, V. E. 2010, Chemie der Erde, 70(1), 7–33.
Hoover, R. B. 2012, Instruments, Methods, and Missions for Astrobiology XV. Proc SPIE, 8521, Article id. 852106.
Hoover, R. B., Rozanov, A. Y., Zhmur, S. I., & Gorlenko, V. M. 1998, Proc SPIE, 3441, 203-216.
Hradil, D., Grygar, T., Hrušková, M., Bezdička, P., Lang, K., Schneeweiss, O. et al. 2004, Clays & Clay Miner., 52(6), 767–778.
Huss, G. R., Rubin, A. E., & Grossman, N. J. 2006, In: Lauretta D. S. & McSween Jr. H. Y. (Eds.), Meteorites and the Early Solar System II., Univ. Arizona Press. http://www.lpi.usra.edu/books/MESSII/9007.pdf.
Hutchison, R., Alexander, C. M. O., & Barber, D. J. 1987, Geochim. Cosmochim. Acta, 51, 1875-1882.
Huang, E., Chen, C. H., Huang, T., Lin, E. H., & Xu, J. A., 2000, Am. Min. 85(3-4), 473-479.
Igisu, M., Ueno, Y., Shimojima, M., Nakashima, S., Awramik, S. M., Ohta, H. et al. 2009, Precambr. Res., 173(1-4), 19-26.
Jones, E. G. & Lineweaver, C. H. 2010, Astrobiol., 10, 3, 349-361.
Juniper, S. K. & Fouquet, Y. 1988, Canadian Miner., 26, 859–869.
Kelemen, S. R. & Fang, H. L. 2001, Energy Fuels, 15, 653–658.
Kerr, P. F. 1952, Clays & Clay Miner., 1, 19–32.
Kerridge, J. F. 1985, Geochim. Cosmochim. Acta, 49, 1707-1714.
Köhler, B., Singer, A., & Stoffers, P. 1994, Clays and Clay Miner., 42, 689-701.
Konhauser, K. O., Hamade, T., Raiswell, R., Morris, R. C. Ferris, F. G., Southam, G. et al. 2002, Geology, 30, 1079–1082.
Konhauser, K. O. 1998, Earth-Science Revs., 43, 91-121.
Konhauser, K. O. & Urrutia, M. M. 1999, Chem. Geol., 161, 399-413.
Kuebler, K. E., Jolliff, B. L., Wang, A. & Haskin, L. A., 2006, Geochim. Cosmochim. Acta, 70(24), 6201-6222.
Kurat, G. 1969, Proceedings of a Symposium on Meteorite Research (7–13 August 1968, Vienna, Austria), Millman P. M (Ed.), Meteorite Research, Springer, Dordrecht, 185-190.
Lane, M. D., Glotch, T. D., Dyar, M. D., Pieters, C. M., Klima, R., Hiroi, T.et al. 2011, Journal of Geophysical Research: Planets, 116(E8).
Madejova, J. & Komadel, P. 2001, Clays & Clay Miner., 49(5), 410-432.
Mapelli, C., Castiglioni, C., Zerbi, G., & Mullen, K. 1999, Phys. Revs B, 60, 12710-12725.
Markovski, C., Byrne, J. M., Lalla, E., Lozano-Gorrín, A. D., Klingelhoefer, G., Rull, F. et al. 2017, Icarus, 296, 49-58.
Mason, B. 1963, Geochim. Cosmochim. Acta, 27, 1011-1023.
Matrajt, G., Muñoz, G. M., Dartois, C. E., d'Hendecourt, L., Deboe, D., & Borg, J. 2005, Astron. & Astrophys., 433, 979–995.
McKay, D. S. Gibson, E. K. Jr, Thomas-Keprta, K. L., Vali, H., Romanek, C. S., Clemett, S. J. et al. 1996, Science, 273(5277), 924-930.
McSween, H. Y. Jr 1979, Rev Geophy. Space Phys., 17, 1069-1078.
Menzies, O. N., Bland, P. A., Berry, F. J., & Cressey, G. 2005, Met. & Planet. Sci., 40, 1023-1042.
Meunier, S. 1871, Compte rendus index, 73, 346-350 (in French).
Müller, C. M., Pejcic, B., Esteban, L., Delle Piane, C., Raven, M., & Mizaikoff, B., 2014, Sci. Reps, 4, 6764.
Nagy, B., Frederiksson, K., Urey, H. C., Claus, G., Andersen, C. A., & Percy, J. 1963, Nature 198, 121-125.
Orlov, A. S., Mashukov, V. I., Rakitin, A. R., & Novikova, E. S. 2012, J. Appl. Spectr., 79(3), 484-489.
Oró, J., Gibert, J., Lichtenstein, H., Wikstrom, S., & Flory, D. A. 1971, Nature, 230, 105-106.
Ostrowski, D. R., Lacy, C. H. S., Gietzen, K. M., & Sears, D. W. G. 2011, Icarus, 212, 682-696.
Parikh, S.J. & Chorover, J. 2006, Langmuir, 22, 8492-8500.
Peng, X., Zhou, H., Wu, Z., Jiang, L., Tang, S., Yao, H. et al. 2007, Chinese Science Bulletin, 52(3), 367-379.
Polgári, M., Gyollai, I., & Bérczi, Sz. 2018, In: Nagy M., McIntosh R. (Eds.), Comprehensive Research on Kaba Meteorite, Acta GGM Debrecina Geology, Geomorphology, Physical Geography Series, Debrecen University Press, Special Issue, 55-69.
Polgári, M., Gyollai, I., Bérczi, Sz., Veres, M., Gucsik, A., Pál-Molnár, E. 2017, In: Europeaan Astrobiology Network Association 2017 (14-17, August, 2017, Aarhus, Denmark), Conference Abstract Book, 55-56.
Polgári, M., Hein, J. R., Tóth, A. L., Pál-Molnár, E., Vigh, T., Bíró, L. et al. 2012, Geology, 4(10), 903-906.
Préat, A., Mamet, B., De Ridder, C., Boulvain, F., & Gillan, D. 2000, Sed. Geol. 137, 107-126.
Rajasekar, A., Maruthamuthu, S., Muthukumar, N., Mohanan, S., Subramanian, P., & Palaniswamy, N. 2006, Corros. Sci., 47, 257–271.
Schopf, J. W., Kudryavtsev, A. B., Czaja, A. D., & Tripathi, A. B. 2007, Precambr. Res., 158, 141-155.

Scott, E.R.D., Krot, A.N., Browning, L.B. 1997, In: Zolensky M., Krot A., & Scott E. R. D. (Eds.), Workshop on Parent-Body and Nebular Modification of Chondritic Materials (17-19 July 1997, Maui, Hawai'i, USA), LPI Technical Report, LPITR 97-02, Houston, TX: Lunar and Planetary Institute, 56.

Srinivasan, P. S. 1935, Proc. Ind. Acad. Sci. - Section A, 2(2), 105-112.

Tuinstra, F. & Koenig, J. L. 1970, J. Chem. Phys., 53(3), 1126-1130.

Urey, H. C. & Craig, H. 1953, Geochim. Cosmochim. Acta, 4, 36-82.

Van Schmus, W. R. & Wood, J. A. 1967, Geochim. et Cosmochim. Acta, 31, 747-765.

Veres, M., Tóth, S., & Koós, M. 2006, Diamond & Relat Mater, 17, 1692-1696.

Watanabe, S., Yamanaka, M., Sakai, A., Sawada, K., & Iwasa, T. 2008, Mater Trans., 49(4), 874- 878.

Wopenka, B. & Pasteris, J.D. 1993, Amer. Miner., 78(5-6), 533-557.

Zhao, J., Zhu, H., Wu, Y., Jian, R., & Wu, G. 2010, Chin. J. Polymer. Sci., 28(3), 385-393.

Zolensky, M. & McSween, H. Y. Jr 1988, In: Kerridge J. F. & Matthews M. S. (Eds.), Meteorites and the Early Solar System, University of Arizona Press: Tucson, 114-143.